MALAYSIAN JOURNAL OF MICROSCOPY

Journal homepage: https://malaysianjournalofmicroscopy.org

RESEARCH ARTICLE

ENHANCED CONDUCTIVITY OF HOLE TRANSPORT LAYERS VIA NICKEL OXIDE AND GRAPHENATED-CARBON NANOTUBE (G-CNT) COMPOSITES

Nurbahirah Norddin[1,2,3], Suhaidi Shafie[1,2,*], Muhammad Idzdihar Idris[3], Mohd Nizar Hamidon[1,2], Fauzan Ahmad[4], Xinzhi Liu[1,2]

[1]*Institute of Nanoscience and Nanotechnology, Universiti Putra Malaysia, 43400 Serdang, Selangor, Malaysia.*
[2]*Department of Electrical and Electronic Engineering, Faculty of Engineering, Universiti Putra Malaysia, 43400 Serdang, Selangor, Malaysia.*
[3]*Faculty of Electronics and Computer Engineering, University Technical Malaysia Melaka (UTeM), 75450 Melaka, Malaysia*
[4]*Malaysia–Japan International Institute of Technology (MJIIT), Universiti Teknologi Malaysia, Jalan Sultan Yahya Petra, 54100 Kuala Lumpur, Malaysia*

Abstract. Perovskite solar cells represent a highly promising renewable energy technology due to their exceptional efficiency and cost-effectiveness. However, limitations exist in commonly used hole transport layers (HTLs) like Spiro-OMeTAD and PEDOT: PSS, which have their drawbacks. Nickel oxide (NiO) is a potential alternative HTL material but suffers from high resistivity which involves low carrier concentration, defect density, and poor charge mobility. In this study, the influence of a graphenated carbon nanotube (g-CNT) mixture on the physical, electrical, and surface morphological properties of NiO thin films was investigated. NiO:g-CNT were synthesized using a sol-gel method and characterized by field emission scanning electron microscopy (FESEM) to analyze surface morphology, X-ray diffraction (XRD) for structural properties, and energy-dispersive X-ray spectroscopy (EDX) for elemental analysis. Electrical properties were measured using a four-point probe to assess conductivity. The results revealed that incorporating 0.5 wt% g-CNT into NiO significantly reduced the resistance of the thin films from 255 kΩ to 67 kΩ. This improvement is attributed to the g-CNT's ability to bridge grain boundaries, enhancing charge transport, even though the crystallite size was smaller compared to pristine NiO. These findings suggest that NiO could improve the performance of perovskite solar cells by enhancing their conductivity.

Keywords: Perovskite, nickel oxide, graphenated-carbon nanotubes, electrical conductivity

Article Info

Received 2 November 2024
Accepted 2 December 2024
Published 6 December 2024

***Corresponding author: suhaidi@upm.edu.my**

ISSN: 1823-7010, eISSN: 2600-7444

1. INTRODUCTION

Renewable energy research become one of the sustainable development goal (SDG) target that created by the United Nations to ensure access to affordable, reliable, sustainable and modern energy for all. The release of pollutants resulting from the burning of fossil fuels constitutes the primary driver of global warming [1]. Renewable energy such as wind turbines, hydroelectric, solar energy and tidal energy can be used to reduce the pollutant which can reduce global warming. Solar energy stands out as a leading renewable source due to its resource-free, pollution-free nature, making it a sustainable solution for the future [2]. However, despite being the dominant technology since the inception of solar energy, silicon-based solar cells have faced significant challenges which are their high cost, complex manufacturing processes, and the generation of toxic. Researchers are actively exploring various solar technologies, including second generation of solar cells consisting of cadmium telluride (CdTe), and copper-indium gallium diselenide (CIGS) generation thin-film offer cost-effectiveness, but have efficiency limitations. In contrast, third-generation solar cells, such as dye-sensitized, organic, and perovskite cells, have emerged as highly efficient and affordable alternatives.

Although the Spiro-OMeTAD as a hole transport layer has shown superior efficiency but the problem associated with its role in perovskite layer degradation and its morphological deformation at higher temperatures causes constraints in the commercialization of perovskite solar cells [3]. Among the organic hole transport layers, poly (3,4- ethylene dioxythiophene): poly (4-styrene- sulfonate) (PEDOT: PSS) is known as the most used one, however, its hygroscopic and acidic nature was found to be detrimental for the device stability.

Nickel oxide (NiO) is a promising candidate for hole transport layer (HTL) in perovskite solar cells due to its advantages like low cost and good stability [2,4]. However, its intrinsic limitations, such as high resistance that hinders efficient charge extraction [5], have hampered its widespread adoption. A mixture of NiO with graphenated-carbon nanotubes (g-CNT) presents a compelling strategy to address this challenge. Carbon nanotubes (CNT) have been used to enhance the electrical conductivity of electronic materials such as in [6] transistors, sensors and batteries. CNTs possess exceptional electrical conductivity, and their incorporation into NiO has the potential to create a composite material with significantly improved conductivity while maintaining the desirable properties of NiO for HTL applications [3,7]. This research investigates the impact of CNT mixture on physical and the electrical properties of NiO, specifically focusing on the changes in resistivity and their correlation with the microstructure and morphology of the resulting composite thin films. By understanding the interplay between mixture and material characteristics, we aim to optimize the development of NiO:g-CNT composites as efficient HTLs for high-performance perovskite solar cells.

2. MATERIALS AND METHODS

The materials used to synthesis Nickel Oxide (NiO) were supplied from the following providers: nickel (II) acetate tetrahydrate (98%) Sigma Aldrich, ethyl alcohol (95%), Isopropyl alcohol (IPA) and Potassium hydroxide (KOH) were purchased from Chemiz (M) Sdn Bhd. Graphenated-carbon nanotubes (g-CNT) from [8] using a floating catalyst chemical vapour deposition (FCCVD) method and formed a bulk-cotton-like structure. The plain glass used in this study is manufactured by the HmbG brand. Deionized water was used to prepare all aqueous solutions.

2.1 Nickel Oxide Synthesis

Initially, the glass is precisely divided into pieces measuring 1.5 x 2.0 cm using a glass cutter. Subsequently, the glass was cleansed using tap water and detergent. Next, the glass was immersed in distilled water (DI) for a duration of 10 minutes and afterward placed in an ultrasonic cleaner. Next, soak with acetone for 10 minutes and put into ultrasonic cleaner then lastly soak with Isopropyl alcohol (IPA) for 10 minutes and put into ultrasonic cleaner. The NiO thin film precursor was prepared by dissolving 0.625 g nickel acetate tetrahydrate ($Ni(OCOCH_3)_2 \cdot 4H2O$) as precursor in the mixture of

ethanol (15 ml) and isopropyl alcohol (10 ml) as solvent. Subsequently, 0.56 g of potassium hydroxide (KOH) was added with 100 ml of deionized water at room temperature. The mixture was added dropwise to obtain the pH of the solution at the value of 11. As mentioned in [9] ph 11 is employed due to the fact that the outcomes demonstrate significant efficiency. The crystalline structure and particle size of NiO can be affected by changes in pH during synthesis. Larger particles often develop at higher pH levels, whereas smaller particles typically form at lower pH values. After that, the temperature rises to 60 ˚C and the pH of the solution is recorded. The pH during the preparation can influence how the materials behave under thermal stress, affecting their performance in catalytic applications [10]. At 60 °C, hydrolysis and condensation reactions occur at an optimal rate, promoting stable sol formation and controlled gelation, which is crucial for uniform NiO films [11]. The solution was then stirred for 2 hours at 60 ºC. After that, the solution is allowed to stand undisturbed at ambient temperature, resulting in the visible separation of the upper portion (supernatant) and lower portion (precipitate) of the combination. Next, eliminate the upper portion of the solution that is floating above. Then the solution was put into Joanlab high-speed centrifuge with a speed 1000 rpm for 10 minutes. The solution is also separated into two parts that is the top part (supernatant), and the bottom part (precipitate) of the mixture. The solution was measured for pure NiO pH 11 and 0.5wt% (0.03 g) of g-CNT in 1ml of Nickel Oxide was added and put in ultrasonic for better dissolve. As mentioned in [3], the solution concentration was 35 mg/ml and 5wt% of CNT and the density of nickel oxide that is 6.67 g/ml was used for this calculation. The spin coat is carried on at 3000 speed for 15 seconds for pure NiO and 0.5wt% NiO:g-CNT. The flowchart for nickel oxide sol-gel synthesis method is shown in Figure 1.

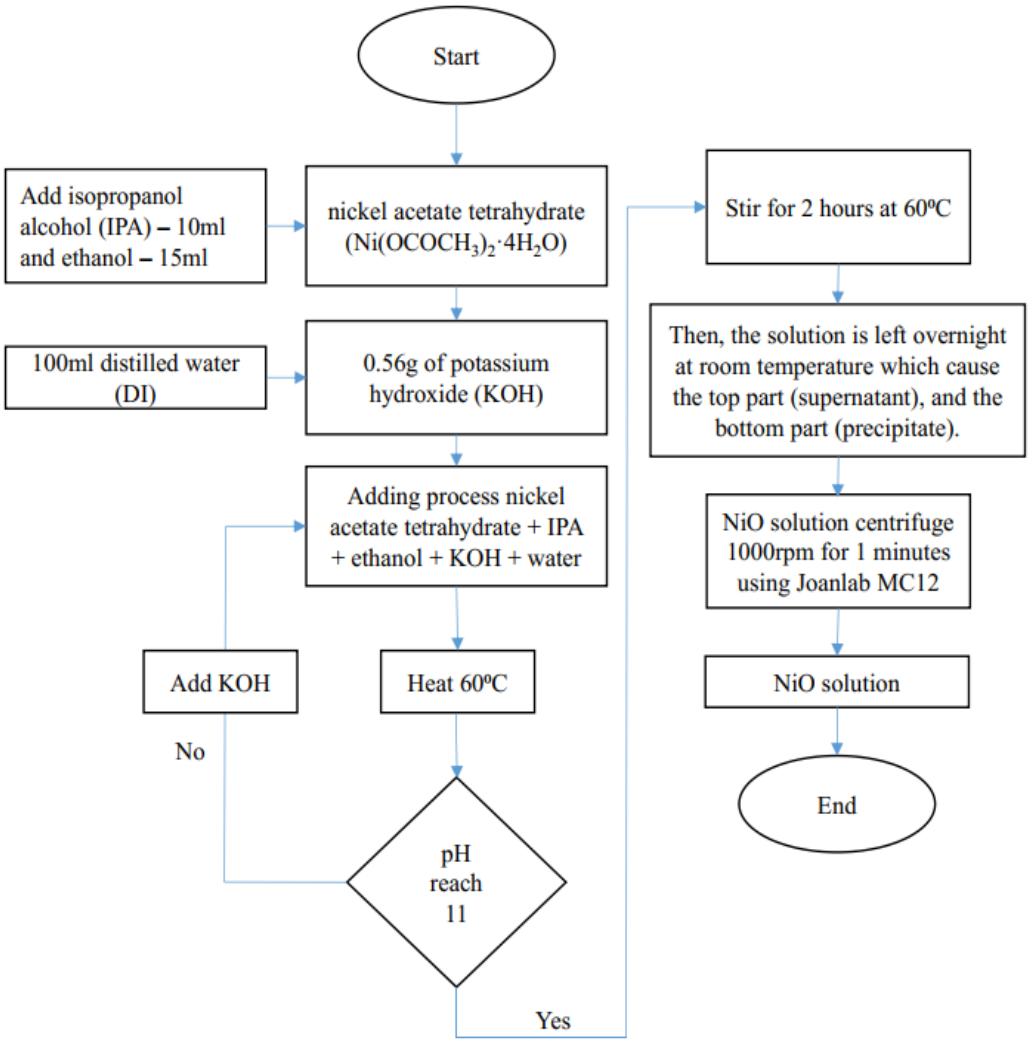

Figure 1: Flowchart of Nickel Oxide sol-gel synthesis

3. RESULTS AND DISCUSSION

3.1 Morphological Study of g-CNT Analysis

Figure 2 shows TEM images for g-CNT came together to create a cotton structure by forming longer, threadlike structures that are entangled with one other. The g-CNTs that were produced had foliates that were perpendicularly oriented and developed from the sidewalls of multiwall CNTs, as indicated by an average diameter of 40 nm [8].

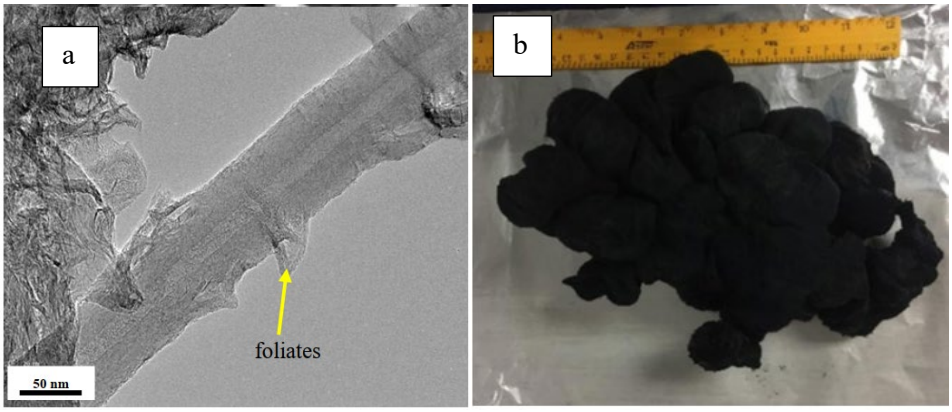

. **Figure 2:** (a) TEM images of g-CNT and (b) optical micrograph as-synthesized g-CNT [8]

The morphology from Schottky Field Emission Scanning Electron Microscope SU5000 (Hitachi) of the graphenated-carbon nanotubes (g-CNT) is shown in Figure 3(a1) and (a2). The samples first were sputter coater with a thin conductive coating (e.g., gold, platinum, or carbon) to prevent charging under the electron beam. Samples were securely mounted on metal stubs with conductive adhesives to ensure good electron conduction. FESEM at lower beam voltages (5 kV) provides enhanced surface details, making it ideal for imaging delicate or soft materials, with clear morphological features observed at magnifications of 2k and 50k. Only 0.5 wt.% of g-CNT was used in 1ml Nickel Oxide. The g-CNT are randomly knotted and cross-linked. It can be seen that the structure appears to consist of large, sheet-like or fibrous networks, suggesting that the features are relatively larger in size compared to pristine Nickel oxide.

Figure 3(b1) and (b2) show the FESEM image of a pristine NiO spin coat on a thin film which has been annealing at 400 ºC for 1 hour. Nickel Oxide structure appears to consist of smaller, granular particles average size of around 0.1 µm. These particles seem tightly packed, and their size is likely on the order of tens to a few hundred nanometers, which is smaller compared to g-CNT. The g-CNT are distributed in the NiO which have been annealing at 400 ºC for one hour and form an interconnected network that is beneficial for improving the electrical conductivity of the composite, as shown in Figure 3(c1) and (c2).

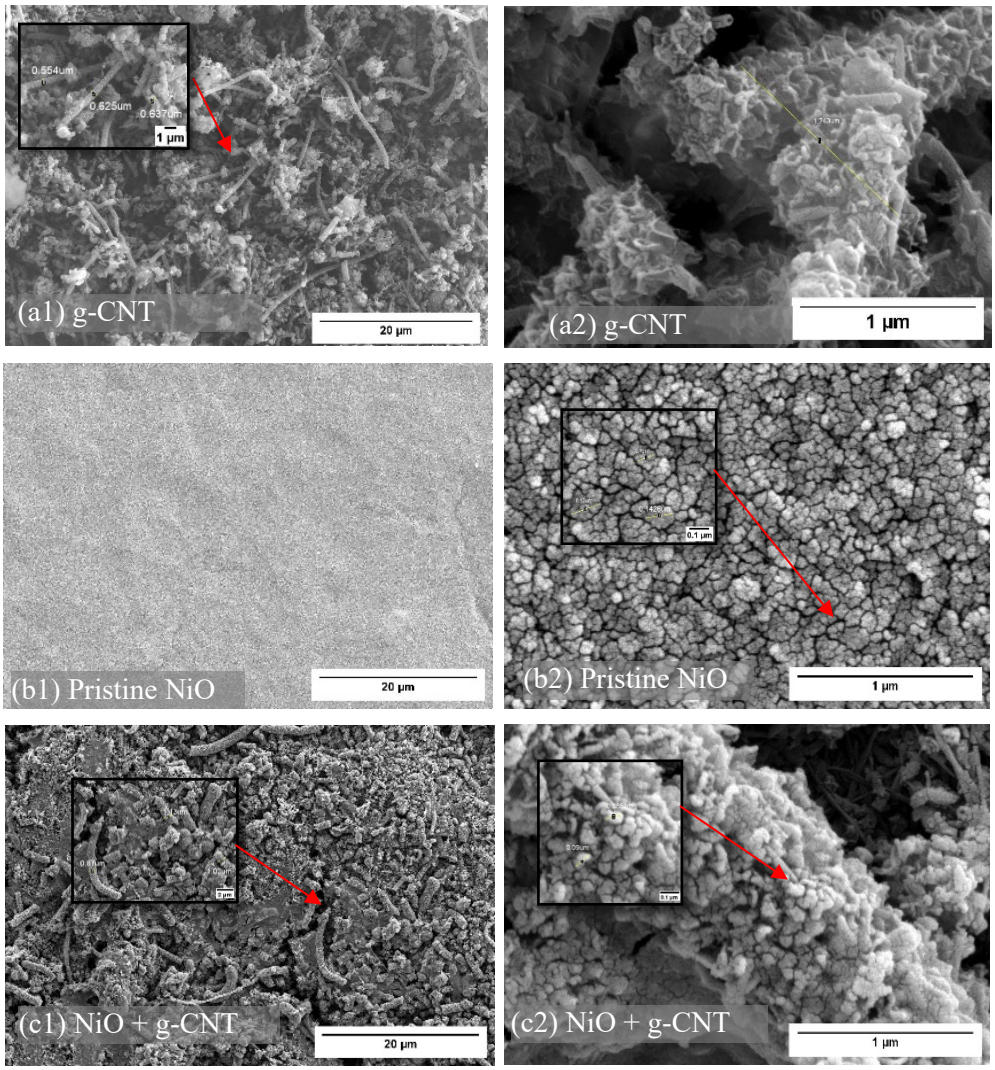

Figure 3: FESEM of thin film (a1,a2) g-CNT, (b1,b2) pristine NiO and (c1,c2) NiO:g-CNT

NiO and NiO:g-CNT thin film is validated using energy dispersive X-ray spectroscopy energy (EDX) shown in Figure 4(a) and (b). The EDX spectra confirmed the existence of nickel and oxide elements on the thin film in Figure 4(a). Then, Figure 4(b) shows the existence of carbon, nickel and oxide. In order to comprehend the basic characteristics and their uses, these results can be useful. As mentioned before, the g-CNT peak was not detected by XRD because of the small amount and beyond the detection limit of XRD in detecting the low content with full continuous scanning but carbon element is shown in EDX in Figure 4(b).

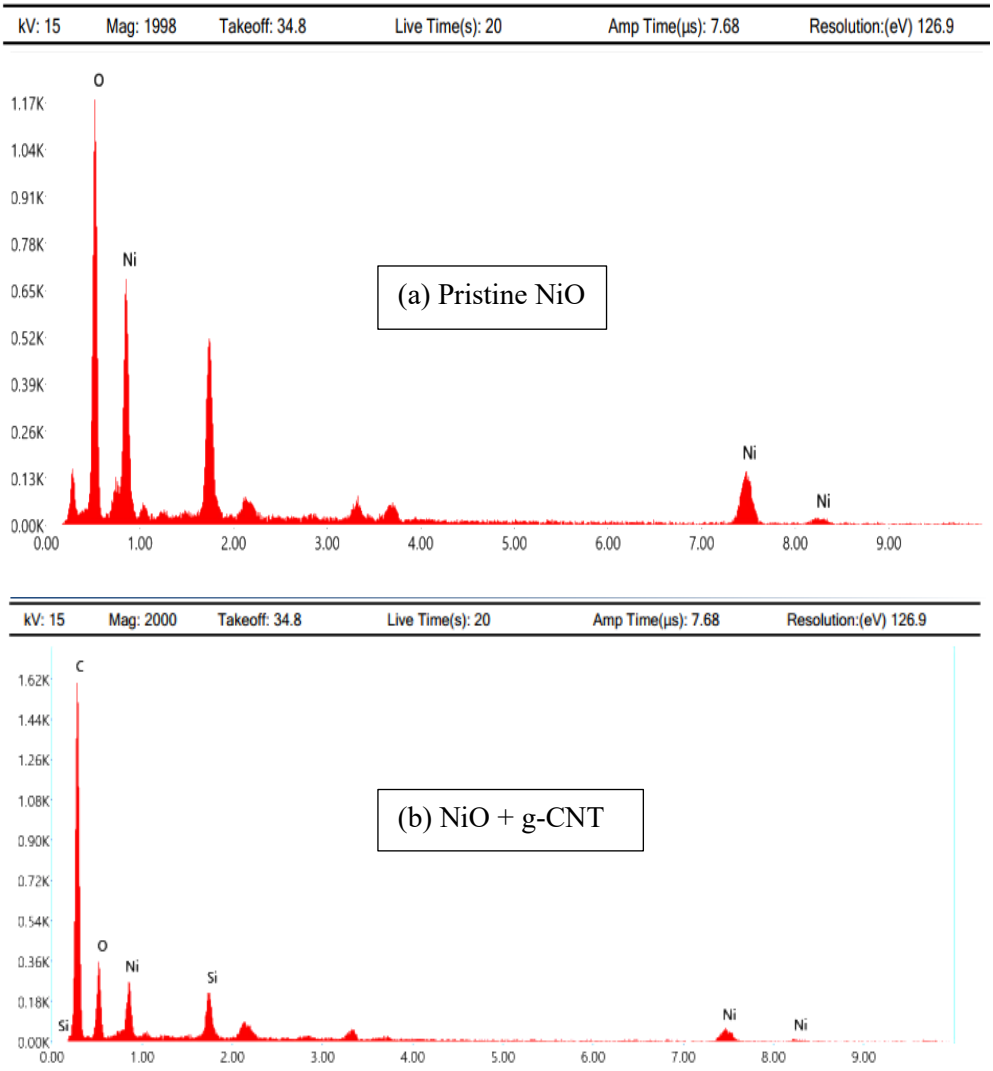

Figure 4: (a) EDX for Nickel Oxide (NiO) and (b) EDX for Nickel Oxide mixed g-CNT (NiO:g-CNT)

3.2 X-ray Diffraction (XRD)

X-ray diffraction (XRD) is a widely used technique for figuring out a material's crystallographic structure. It operates by first applying incident X-rays to a sample, after which the intensities and scattering angles of the X-rays that escape the material are measured. Through the analysis of the angles and intensities at which the diffracted X-ray beams contact with the material, XRD offers comprehensive insights into the material's physical, chemical, and crystallographic characteristics [12]. In this investigation, samples were generated with incident X-rays to generate an XRD pattern of NiO at pH levels 11, with λ=1.54 A and angle of incident ranging from 20º to 90º. The positions of the atoms in the lattice planes were used to evaluate the intensities and scattering angles. The XRD graph for Nickel Oxide shows the crystalline type of material. The XRD of the Nickel Oxide (NiO) is shown in Figure 5. The diffraction peaks at 37.249º, 43.276º, and 62.879º correspond to (111), (200) and (220) planes. Two minor peaks at 75.416º, and 79.409º, are related to (311) and (222) planes. These results are in agreement with the reference JCPDS card no. 47–1049 [3,12]. The g-CNT peak was not detected by XRD because of the small amount and beyond the detection limit of XRD in detecting the low content with full continuous scanning [13]. As shown in [3] the peak is shown at (0 0 2) at 20º – 35º with the weight CNT of 5wt%. However, carbon is visible in the EDX displayed in Figure 4(b) but not in the XRD.

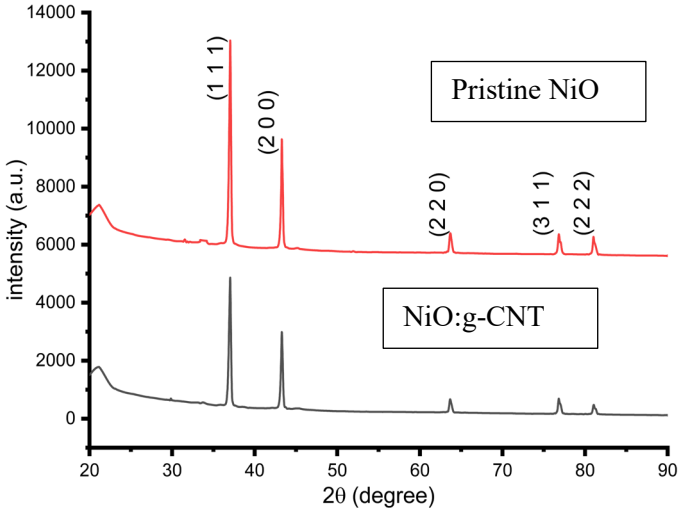

Figure 5: XRD of the Nickel Oxide (NiO) nanoparticle

The crystallite size in equation (1) for the prepared NiO was estimated by taking crystalline size calculated intense peaks at 37.249º, 43.276º, and 62.879º using the Debye-Scherrer equation [14-15]

$$D = \frac{K}{\beta coscos\,\theta} \quad (1)$$

where:

K = 0.9 = Scherrer's constant,
λ = wavelength of X-rays,
β = full width at half-maximum (FWHM) of the diffraction peak,
θ = Bragg diffraction angle.

X-ray diffraction data (XRD) computations yield a dislocation density that is more accurate for a specific powder region. Its evaluation of dislocation density was done using Equation (2).

$$\delta=1/D\text{^}2 \quad (2)$$

In order to gain insight into the deformations and defects of the grains in the produced films, the lattice strain (ε) can be determined using equation (3). The summary findings are presented in Table 1.

$$\varepsilon=\beta/(4\tan\theta) \quad (3)$$

Enhanced grain boundaries caused by smaller crystallites can occasionally obstruct conductivity. Grain boundaries are areas that exist between crystallites, characterized by a lower degree of structural organization in the crystal lattice. These flaws have the potential to interrupt the movement of electrons. The size of crystallites can have an impact on the absorption and scattering of light. The precise impacts will vary according to the composition and dimensions of the crystallites. Smaller crystallites typically result in a higher number of grain boundaries. Even though the crystallite size for NiO:g-CNT is smaller than NiO, graphenated-carbon nanotubes (g-CNT) have the potential to connect these grain boundaries, therefore establishing more efficient routes for charge carriers to cross the material [16]. This may reduce the negative effect of enhanced grain boundaries often connected to reduced crystallite size. The features, including position angle, full width at half maximum (FWHM), and crystallite size, are compiled in Table 1 to examine the impact of g-CNT on Nickel Oxide.

Table 1: The average crystallite size (D), dislocation density (δ), and lattice strain function (ε) of the characteristic peaks

Material	hkl	2θ (degree)	FWHM	Average crystallite size, D (nm)	Average dislocation density $\delta x10^{-3}(nm^{-2})$	Average microstrain , ε
NiO	1 1 1	37.05	0.239	43.03638914	0.560788696	1.820684534
NiO+g-CNT	1 1 1	37.04	0.2637	40.34506416	0.647284072	1.977982585

3.3 Electrical Analysis

The annealing temperature of both pure NiO and NiO mixed with g-CNT is 400 °C. This is because [17] mentions that excellent optical and electrical characteristics can be obtained at annealing temperatures exceeding 300 °C. It is shown that the resistance for NiO mixed with g-CNT is decreased to 67 KΩ from 255 KΩ when 0.5wt% g-CNT added into the NiO solution. Linear four-point probe illustration is shown in Figure 6. The thickness of the Nickel Oxide thin film achieved using 3000 rpm for 15 seconds is 60 nm or 60 µcm [18-19]. The electrical conductivity of graphenated carbon nanotube (g-CNT) is high in the range of $1.28x10^{-3}$– 6.45 $x10^{-3}$ Scm^{-1} [8]. Thus, the benefits of CNT's high conductivity allow for a reduction in Nickel Oxide resistance. The conductivity of nickel oxide alone is significantly lower due to its inherently high resistivity as mentioned by Patil [20] that resistivity value at 1 $x10^{4}$ – $9x10^{4}$ Ωcm which makes the conductivity at $0.3x10^{-3}$ Scm^{-1} to 0.011 $x10^{-3}$ Scm^{-1}.

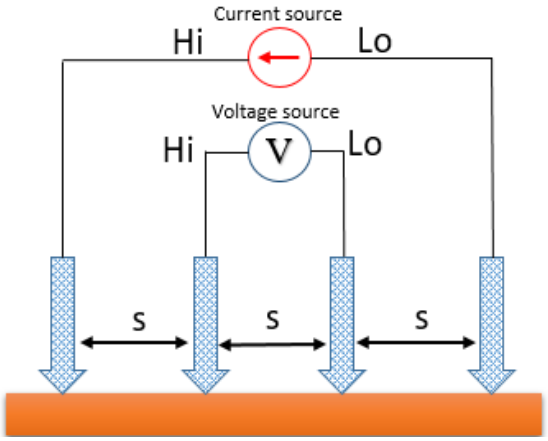

Figure 6: Linear four-point probe illustration

The results of the measurement obtained from the linear four-point probe are shown in Table 2. The sheet resistance was calculated using equation (5), resistivity using equation (6) and conductivity using equation (7).

$$\rho_{\square}(\Omega\square^{-1}) = \frac{\pi}{ln(2)}\frac{V}{I} = 4.5324\frac{V}{I}[\Omega\square^{-1}] \quad (5)$$

$$\rho = \rho_{\square}t \quad (6)$$

$$\sigma = \frac{1}{\rho} \quad (7)$$

Table 2: Measurement obtained from the linear four-point probe

HTL	Resistance (KΩ)	Sheet Resistance (MΩ□$^{-1}$)or(MΩ.cm-^{2})	Resistivity (Ω.cm)	Conductivity (σ) (S.cm^{-1})
Pristine NiO ph11	255.5	1.2190	7.2	0.138
g-CNT 0.5 wt%	67.284	0.3138	1.86	0.538

4. CONCLUSIONS

The synthesis of Nickel Oxide can be achieved by the sol-gel method synthesis, and its elemental composition has been confirmed using X-ray diffraction (XRD) and energy-dispersive X-ray spectroscopy (EDX). Subsequently, the process of enhancing conductivity in Nickel Oxide by utilizing graphenated carbon nanotubes (g-CNT) can be demonstrated. Conductivity can be occasionally reduced by enhanced grain boundaries resulting from smaller crystallites. Graphenated carbon nanotubes (g-CNT) can connect these grain boundaries, so creating more effective pathways for charge carriers to cross the material, even if the crystallite size for NiO:g-CNT is less than that of NiO. This demonstrates how adding 0.5 wt% of g-CNT to the NiO solution causes the resistance for NiO mixture with g-CNT to reduce to 67 KΩ from 255 KΩ and increases the conductivity of Nickel Oxide. The enhancement of conductivity will undoubtedly contribute to improving the quality of Nickel Oxide used in the hole transport layer of perovskite solar cells.

Acknowledgements

This study is funded by the Ministry of Higher Education (MOHE) of Malaysia through the Fundamental Research Grant Scheme (FRGS), No. FRGS/1/2022/TK07/UTEM/02/17. The authors would like to thank Universiti Teknikal Malaysia Melaka (UTeM) and Universiti Putra Malaysia (UPM) for all their supports.

Author Contributions

All authors contributed toward data analysis, drafting and critically revising the paper and agree to be accountable for all aspects of the work.

Disclosure of Conflict of Interest

The authors have no disclosures to declare

Compliance with Ethical Standards

The work is compliant with ethical standards

References

[1] Bist, A., Pant, B., Ojha, G. P., Acharya, J., Park, M. & Saud, P. S. (2023). Novel materials in perovskite solar cells: Efficiency, stability, and future perspectives. *Nanomaterials*, 13(11), 1724.

[2]Hassan, Q., Viktor, P., Al-Musawi, T. J., Mahmood, A. B, Algburi, S., Alzoubi, H. M., Khudhair Al-Jiboory, A., Sameen. A. Z., Salman, H. M. & Jaszczur, M. (2024). The renewable energy role in the global energy transformations. *Renewable Energy Focus*, 48, 100545.

[3] Kartikay, P., Sadhukhan, D., Yella, A. & Mallick, S. (2021). Enhanced charge transport in low temperature carbon-based n-i-p perovskite solar cells with NiOx-CNT hole transport material. *Solar Energy Materials and Solar Cells*, 230, 111241.

[4] Tahir, M., Abd-ur-Rehman, H. M., Khoja, A. H., Anwar, M., Mansoor, A., Abbas, F. & Shakir, S. (2024). Praseodymium doped nickel oxide as hole-transport layer for efficient planar perovskite solar cells. *Optik*, 300, 171630.

[5] Liu, J., Yin, X., Guo, Y., Que, M., Chen, J., Chen, Z. & Que, W. (2020). Influence of hole transport layers/perovskite interfaces on the hysteresis behavior of inverted perovskite solar cells. *ACS Applied Energy Materials*, 3(7), 6391–6399.

[6] Abdulhameed, A., Wahab, N. Z. A., Mohtar, M. N., Hamidon, M. N., Shafie, S. & Halin, I. A. (2021). Methods and applications of electrical conductivity enhancement of materials using carbon nanotubes. *Journal of Electronic Materials*, 50(6), 3207–3221.

[7] Mustafa, K. A. M., Al-Mousoi, A. K., Singh, S., Kumar, A., Hossain, M. K., Salih, S. Q., Sasikumar, P., Pandey, R., A.Yadav, A. & Yaseen, Z. M. (2023). Improving the performance of perovskite solar cells with carbon nanotubes as a hole transport layer. *Optical Materials*, 138, 113702.

[8] Yusuf, Y., Shafie, S., Ismail, I., Ahmad, F., Hamidon, M. N., Pandey, S. S., Muhammad, N. Y & Lei, W. (2021). A comparative study of graphenated-carbon nanotubes cotton and carbon nanotubes as catalysts for counter electrode in dye-sensitized solar cells. *Malaysian Journal of Microscopy*, 17(2), 162–174.

[9] Muniandy, S., Idris, M. I., Napiah, Z. A. F. M., Norddin, N., Rashid, M., Zuhdi, A. W. M. & Bradley, L. (2023).The effect of different precursor solutions on the structural, morphological, and optical properties of nickel oxide as an efficient hole transport layer for perovskite solar cells. *Pertanika Journal of Science and Technology*, 31(4), 2047–2066.

[10] Veselov, G. B., Karnaukhov, T. M., Stoyanovskii, V. O. & Vedyagin, A. A. (2022). Preparation of the nanostructured ni-mg-o oxide system by a sol–gel technique at varied pH. *Nanomaterials*, 12(6), 952.

[11] Dhas, S. D., Maldar, P. S., Patil, M. D., Waikar, M. R., Sonkawade, R.G., & Moholkar, A.V. (2022). Sol-gel synthesized nickel oxide nanostructures on nickel foam and nickel mesh for a targeted energy storage application. *Journal of Energy Storage*, 47, 103658.

[12] Omori, N. E., Bobitan, A. D., Vamvakeros, A., Beale, A. M. & Jacques, S. D. M. (2023). Recent developments in X-ray diffraction/scattering computed tomography for materials science. *Philosophical Transactions of the Royal Society A: Mathematical, Physical and Engineering Sciences*, 381(2259), 20220350.

[13] Wakhi Anuar, N. F. B., Omar, M. Z., Salleh, M. S., Zamri, W. F. H & Md Ali, A. (2024). Effect of graphene addition on microstructure and wear behaviour of the A356-based composite fabricated by thixoforming process. *Journal of Materials Research and Technology*, 30, 4813–4831.

[14] Pinzón, C., Martínez, N., Casas, G., Alvira, F. C., Denon, N., Brusasco, G., Medina Chanduví, H., Gil Rebaza, A. V & Cappelletti, M. A. (2022). Optimization of inverted all-inorganic CsPbI3 and CsPbI2Br perovskite solar cells by SCAPS-1D simulation. *Solar*, 2(4), 559-571.

[15] Bonomo, M. (2018). Synthesis and characterization of NiO nanostructures: a review. *Journal of Nanoparticle Research*, 20(8), 222.

[16] Luo, Q., Wu, R., Ma, L., Wang, C., Liu, H., Lin, H., Wang, N., Chen, Y. & Guo, Z. (2021). Recent advances in carbon nanotube utilizations in perovskite solar cells. *Advanced Functional Materials*, 31(6), 2004765.

[17] Ivanova, T. A., Harizanova, M. & Shipochkaand, P. V. (2022). Nickel oxide films deposited by sol-gel method: Effect of annealing temperature on structural, optical, and electrical properties. *Materials,* 15(5), 1742.

[18] Larson, R. G. & Rehg, T. J. (1997). Spin Coating. In *Liquid Film Coating: Scientific Principles and Their Technological Implications*, Ed. Kistler, S. F. & Schweizer, P. M. (Dordrecht: Springer Netherlands), pp. 709–734.

[19] Pichumani, M., Bagheri, P., Poduska, K. M., González-Viñas, W. & Yethiraj, A. (2013). Dynamics, crystallization and structures in colloid spin coating. *Soft Matter*, 9(12), 3220–3229.

[20] Patil, P. S. & Kadam, L. D. (2002).Preparation and characterization of spray pyrolyzed nickel oxide (NiO) thin films. *Applied Surface Science*, 199(1), 211–221.